Optics Communications 449 (2019) 39–44

Contents lists available at ScienceDirect

Optics Communications

journal homepage: www.elsevier.com/locate/optcom

Near-diffraction-limited semiconductor disk lasers

Guanyu Hou [a,b], Lijie Wang [a], Jian Feng [a,b], Andreas Popp [c], Berthold Schmidt [c], Huanyu Lu [a,b], Cunzhu Tong [a,*], Shili Shu [a], Lijun Wang [a]

[a] State Key laboratory of Luminescence and Applications, Changchun Institute of Optics, Fine Mechanics and Physics, Chinese Academy of Sciences, Changchun 130033, China

[b] Center of Materials Science and Optoelectronics Engineering, the University of Chinese Academy of Sciences, Beijing 100049, China

[c] TRUMPF GmbH+Co.KG, Ditzingen 71254, Germany

ARTICLE INFO

OCIS:
140.7270
140.5960
140.5560
140.0140

Keywords:
Semiconductor disk lasers
Beam quality
High power

ABSTRACT

High power semiconductor disk lasers (SDLs) with near-diffraction limited beam quality were demonstrated. The influence of the incident angle, operation temperature, cavity length and curvature radius of the output coupler mirror on the beam quality were investigated. The condition for near-diffraction limited beam quality was analyzed. Choosing the pump spot size 10%–20% smaller than the fundamental mode size is the roughly optimized condition for achieving near-diffraction limited beam quality in SDLs. Finally, the SDL with an output power of 12.9 W and M^2<1.2 was realized.

1. Introduction

Semiconductor disk lasers (SDLs) [1–3], also known as optically pumped vertical external cavity surface-emitting lasers (VECSELs) [4–7], are very attractive for high-power and high beam quality operation. This type of lasers is similar to diode-pumped solid-state lasers but the gain material is semiconductor quantum-wells (QWs) [3–7] or quantum dots [8–10], which takes the advantages of semiconductor lasers, such as the versatile wavelength, wide-pumping wavelength and efficient pump absorption. Many applications require dozens of watts power operating with near-diffraction-limited beam quality. An example is non-linear frequency conversion, which requires TEM_{00} mode (M^2<1.2) to achieve high conversion efficiency [11]. In the area of laser material processing and sensor applications, near-diffraction-limited beam quality allows a small spot with high power density over large distances [12]. The conventional electrically driven edge-emitting semiconductor lasers are limited by the asymmetric and narrow cavity that leads to a high divergence angle and poor beam quality. Although decreasing the width of ridge waveguide is able to realize fundamental mode operation, the output power is restricted to a few watts. Meanwhile, electrically driven vertical-cavity surface-emitting lasers (VCSELs) also suffer from the mode area limitation due to the current injection challenging at large beam areas, which prevents the power exceeding watt level with a fundamental mode [13]. Even for high brightness semiconductor lasers developed by beam combining technology, it is still difficult to obtain near-diffraction-limited beam quality due to the inherent disadvantage of the broad-area waveguide [14,15].

The SDL provides a possible way to conquer the limitations of mode area, which substantially increases the TEM_{00} output power to 0.5 W at the first beginning [4]. Another advantage of SDL is that it is able to scale the optical output power by enlarging the pump area [16] while maintaining high beam quality. In 2006, the SDL with fundamental transverse mode operation were achieved in average output power to ~4 W (M^2<1.15) [17] and ~4.4 W (M^2<1.13) [18]. Although so far the best SDLs in a fundamental transverse mode can achieve more than 20 W output power with $M^2 \leq 1.1$ at 980 nm [13] and 532 nm [19], a detailed study on the limitation factors of the beam quality in SDLs is still lacked.

In this paper, we investigated the effects of the incident angle, operation temperature, cavity length and curvature radius of the output coupler (OC) mirror on the beam quality of a 1030 nm SDL. The mechanism behind was discussed, and the condition for near-diffraction limited beam quality was analyzed.

2. SDL design and setup

Fig. 1(a) shows the structure of the SDL, which is composed of an active region with QWs, distributed Bragg reflector (DBR) mirror and InGaP cap layer. It was grown by metal–organic vapor phase epitaxy (MOVPE) in a reverse order on the GaAs substrate. The DBR mirror is made up of 20 pairs of undoped AlAs/GaAs layers. The active region includes 10 layers of 8 nm InGaAs compressively strained quantum

* Corresponding author.
E-mail address: tongcz@ciomp.ac.cn (C.-Z. Tong).

https://doi.org/10.1016/j.optcom.2019.05.035
Received 16 February 2019; Received in revised form 14 May 2019; Accepted 16 May 2019
Available online 20 May 2019
0030-4018/© 2019 Elsevier B.V. All rights reserved.

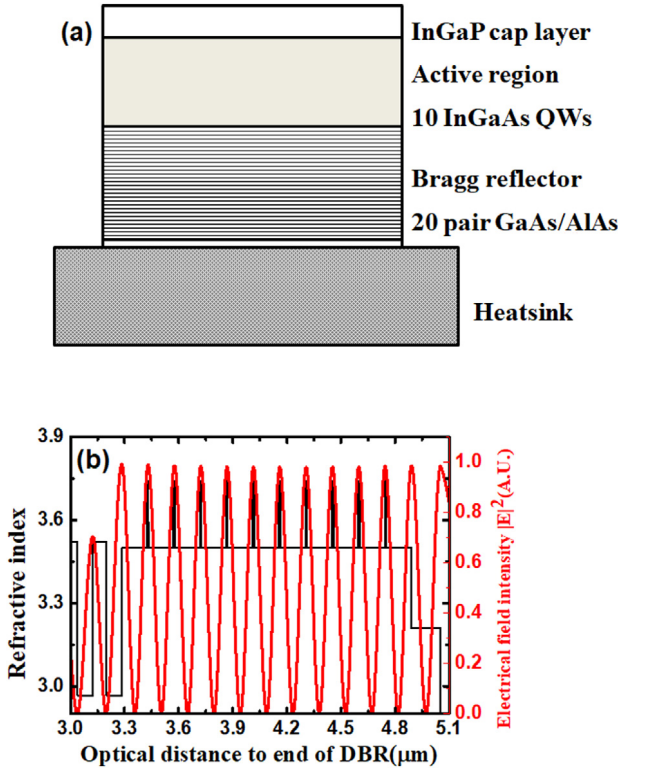

Fig. 1. (a) Schematic diagram of the designed SDL, (b) the refractive index profile and the standing wave distribution in the active region of the designed SDL.

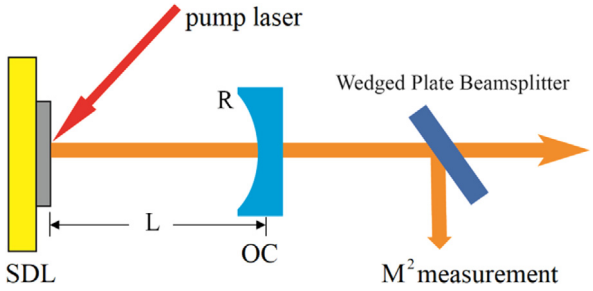

Fig. 2. Schematic diagram of the experimental setup.

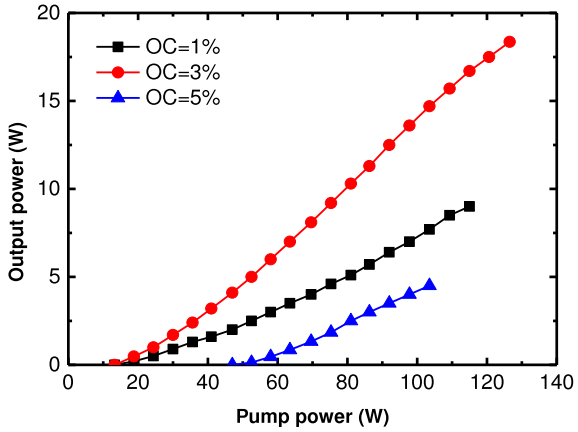

Fig. 3. Pump–Output power characteristics of the SDL for OC mirrors with varying transmittance of 1%, 3% and 5%. The curvature radius of OC mirrors is 100 mm, the cavity length is 70 mm, and the TEC temperature is 10 °C.

wells (QWs) with GaAs barrier and a tensile strained GaAsP layer for strain compensation. Just as shown in Fig. 1(b), those QWs are distributed periodically at the optimized anti-node positions of the standing wave in the optical cavity to ensure a low threshold and homogeneous gain [20]. After that it was a half wavelength InGaP cap layer that prevents carrier diffusing to the chip surface and non-radiative recombining there [21]. The chip was bonded on a diamond heatspreader via the pre-metallized diamond method [22] and the substrate was removed by selective chemical etching. This SDL was designed to emit at around 1030 nm and the active region was optimized for efficient optical pump in the wavelength range of 790 nm–820 nm.

The SDL was optically pumped by an 808 nm fiber-coupled diode laser with a maximum output power of 350 W. Fig. 2 shows the setup of this experiment. The optically-pumped SDL is formed by a simply linear I-shaped cavity with the gain chip as one end mirror and the OC as the external second end mirror. The pump beam is focused into a spot with 600 μm diameter on the SDL surface. As shown in Fig. 2, a wedged plate beam-splitter (550 mm far from the SDL) is used for the measurement of the beam quality to avoid damaging the beam analyzer by the strong laser beam. The distance between the beam analyzer and the beam-splitter is 500 mm. The diamond bonded with SDL chip is attached on a copper heatsink and the temperature is controlled by a thermoelectric cooler (TEC). A water-cooled copper plate is used to dissipate the heat generated in the gain chip and TEC finally.

3. Results and discussion

First, we study the influence of the transmission of the OC mirror on the SDL's output power. For this case, the curvature radius of OC mirrors is fixed at R = 100 mm. However, the transmission of OC mirrors is varied between 1% and 5%. The results are shown in Fig. 3, where the cavity length is about 70 mm and the TEC temperature is set to 10 °C. The pump beam is incident under a 50° angle. A maximum output power of 18.36 W as well as the highest slope efficiency of 17.2% is obtained for 3%-transmission. We use this transmission for all the following measurements.

Next, we investigate the influence of the incident angle of pump beams on the SDL's performance. The OC mirror with R = 250 mm and 3%-transmission was chosen. The cavity length is 110 mm and the TEC temperature is 10 °C. Fig. 4(a) shows the measured output power characteristics under different incidence angles of pump beams. The maximum output power of 18.3 W with the highest slope efficiency of 15.8% is obtained for 30° incident pump beam angle. The beam quality is shown in Fig. 4(b). The M^2 factors are measured by a commercial beam propagation analyzer M2MS-BP209 from Thorlabs company according to ISO11146 standard. At low output power, the M^2 factors increase with output power both in the x and y directions. At higher output power, they slightly decrease with increasing output power. The beam quality in the x direction (M^2_x) is worse than that in the y direction (M^2_y) for the three incident angles. The best beam quality in the x direction is achieved under 30°-incident angle, where M^2_x is 1.98 at the maximum output power. In the y direction, M^2_y under 30°-incident angle is slightly higher than that under 40°-incident angle at 16 W output power. However, smallest difference between the beam quality in x and y directions is obtained under 30°-incident angle. This is due to that the output beam profile under 30°-incident angle is closer to a circular shape as shown in the inset of Fig. 4(a), resulting in a better beam quality.

Subsequently, the impact of TEC temperatures at 10, 15 and 20 °C on the SDL performance is shown in Fig. 5(a) and (b). As can be seen in Fig. 5(a), an obvious improvement for the output power and slope efficiency is observed when the TEC temperature reduces from 20 °C down to 10 °C. Fig. 5(b) shows the effect of the temperature on the beam quality. The temperature of 10 °C seems to maintain a better beam quality in the x direction, and with a smallest difference of the beam quality between x and y directions at higher output power.

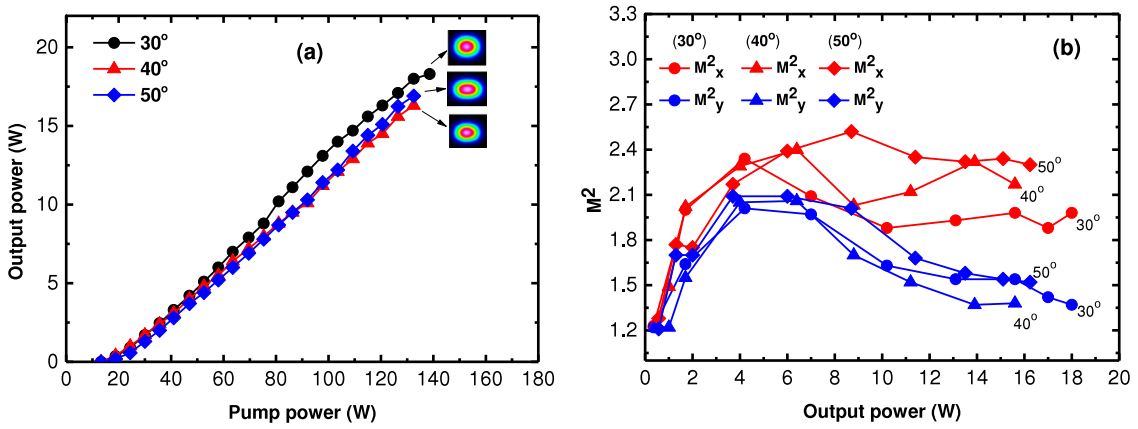

Fig. 4. (a) Pump–Output power characteristics for various pump beam incident angles. Insets: the beam profiles recorded at each maximum output power (b) shows the beam quality of the SDL under the three different pump beam incident angles.

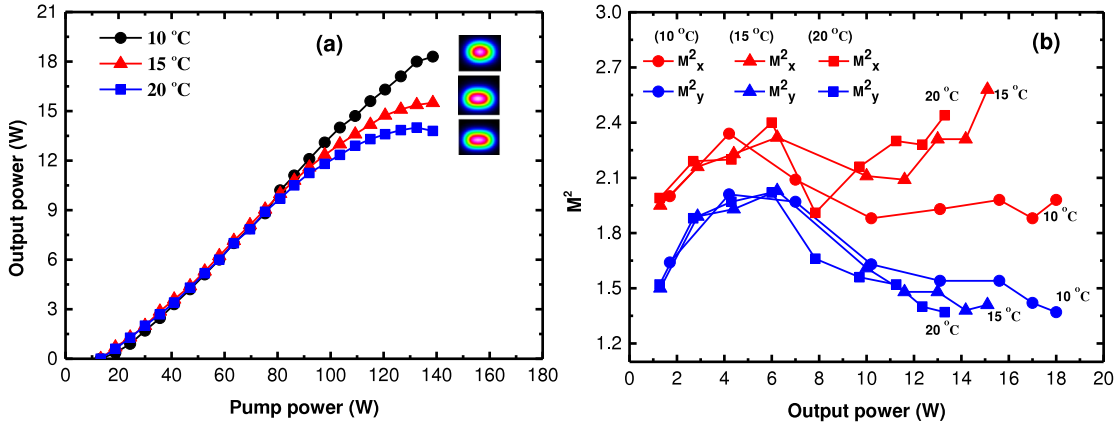

Fig. 5. (a) Pump–Output power characteristics for the curvature radius of 250 mm OC mirror with different TEC temperatures, a cavity length of 110 mm, and the incident angle of pump beam is 30°. Insets: the beam profiles recorded at each maximum output power (b) shows the beam quality of the SDL for different TEC temperatures.

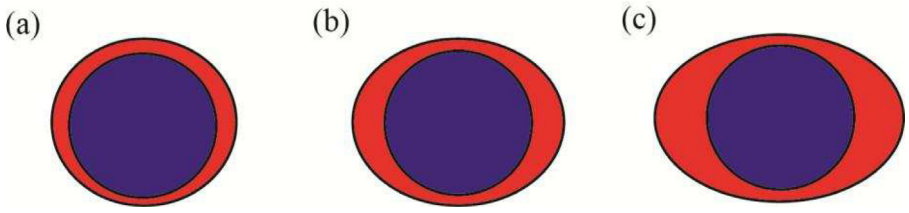

Fig. 6. The presumption about the overlapping situation between the fundamental mode shape (blue circle) and the pump spot (red circle). The incident angle: (a) 30°, (b) 40° and (c) 50° . (For interpretation of the references to color in this figure legend, the reader is referred to the web version of this article.)

From Figs. 4(b) and 5(b) we can see that the M^2 in the y direction is better than the x direction under various angles and temperatures. This is maybe due to the influence of the pump beam profile on the SDL. We guess that the beam profile changes in x direction much quicker than y direction from the 30°to 50°, which leading to the pump spot size matches the cavity mode size with the same tendency (see Fig. 6).

To study the influence of the curvature radius of OC mirrors on the emission power and beam quality of the SDL, three curvature radius R = 100 mm, 250 mm and 1000 mm are selected. Based on above results, we set the incident angle at 30° and the TEC temperature as 10 °C. To simplify the measurement, we measure the maximum output power under 70 W pump power as a function of the cavity length, which is shown in Fig. 7(a), (c) and (e) for three OC mirrors. As can be seen, the lowest output powers occur when the cavity length is equal to a half of the curvature radius. In addition, higher output power can be obtained when the cavity length either increases to the curvature radius or reduces from the half length of the curvature radius. The distance between the OC mirror and the SDL is limited by the mount of the OC mirror, which may block the pump beam when the mirror is very close to the SDL. Therefore, shorter cavity length or the cavity length approaching the OC curvature radius are beneficial for high power output.

We choose two cavity lengths for each OC mirror to investigate the SDL performance. The continuous wave (CW) output power of the SDL with these three different curvature radius R and different cavity lengths L are measured and shown in Fig. 7. Fig. 7(b) presents the results of the SDL with R = 100 mm. The cavity lengths of 30 mm and 60 mm are investigated, in which case the OC mirror is close to the SDL or near the position at a half-length of the curvature radius. As shown in Fig. 7(b), the pump threshold is about 10 W both for the cavity length of 30 mm and 60 mm. The slope efficiency is 16.5% for the cavity length of 30 mm and 15.9% for 60 mm, respectively. The maximum output power is around 20 W under the pump power of 138.6 W, and the maximum optical to optical conversion efficiency (OOE) is 15.6%

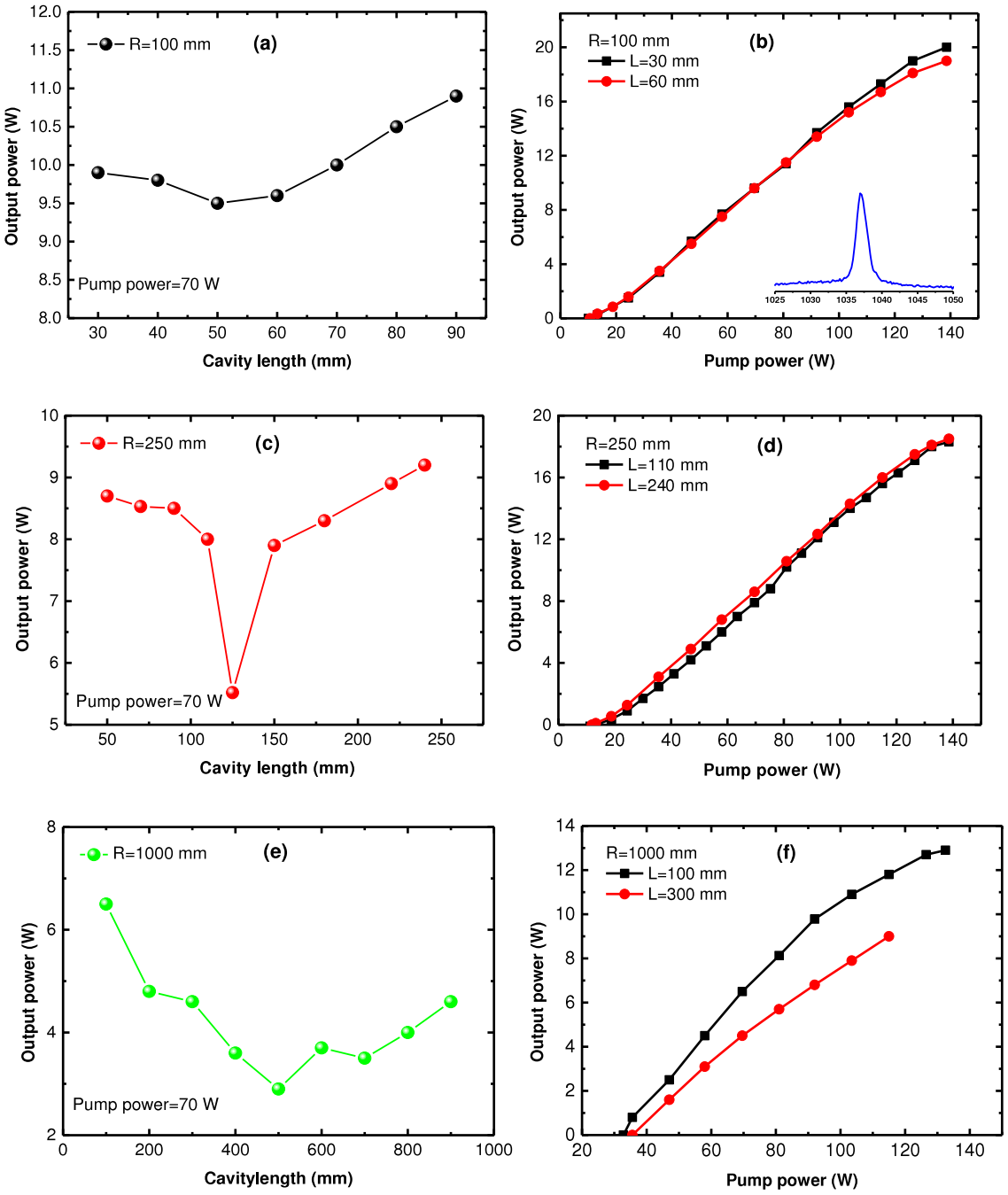

Fig. 7. The maximum output power at the pump power of 70 W for different cavity lengths: (a) R = 100 mm, (c) R = 250 mm and (e) R = 1000 mm. Output power curves of SDLs for (b) curvature radius of OC R = 100 mm with cavity length of 30 mm and 60 mm, (d) R = 250 mm with cavity length of 110 mm and 240 mm, and (f) R = 1000 mm with cavity length of 100 mm and 300 mm. The inset in (b) shows the lasing spectra.

for the cavity length of 30 mm. The maximum output power for the cavity length of 60 mm is 19 W. The inset shows the normalized lasing spectrum. The lasing wavelength is 1037 nm at 40 W pump power.

Fig. 7(d) shows the output power of the SDL versus the pump power with the curvature radius R = 250 mm. For this OC mirror, one cavity length is chosen to be 110 mm (close to a half-length of the curvature radius), and the other is 240 mm (close to the curvature radius). The threshold is about 13.3 W for both cavity length. For the cavity length of 110 mm, the maximum output power and OOE are 18.3 W and 14.6% respectively, while the slope efficiency is 15.8%. For the cavity length of 240 mm, the maximum output power before the thermal roll-over is 18.5 W and the OOE is 14.8%.

Fig. 7(f) illustrates the output power of SDL versus the pump power with the curvature radius R = 1000 mm. To avoid too long cavity, we chose L = 100 mm and 300 mm. It can be seen from Fig. 7(f) that the maximum output power of 12.9 W is achieved at the pump power of 132.5 W for L = 100 mm. For the cavity length of 300 mm, the maximum output power is only 9 W. The maximum OOEs are respectively 12.9% and 11.3% for L = 100 mm and 300 mm.

From above results, it can be found that the maximum output power is 20 W achieved by the OC with R = 100 mm, and the pump threshold is as low as 10 W.

The beam quality of the SDL with different OC mirrors and cavity lengths are measured in Fig. 8. The M^2 factors of the SDL with R = 100 mm are plotted in Fig. 8(a) as a function of output power. The

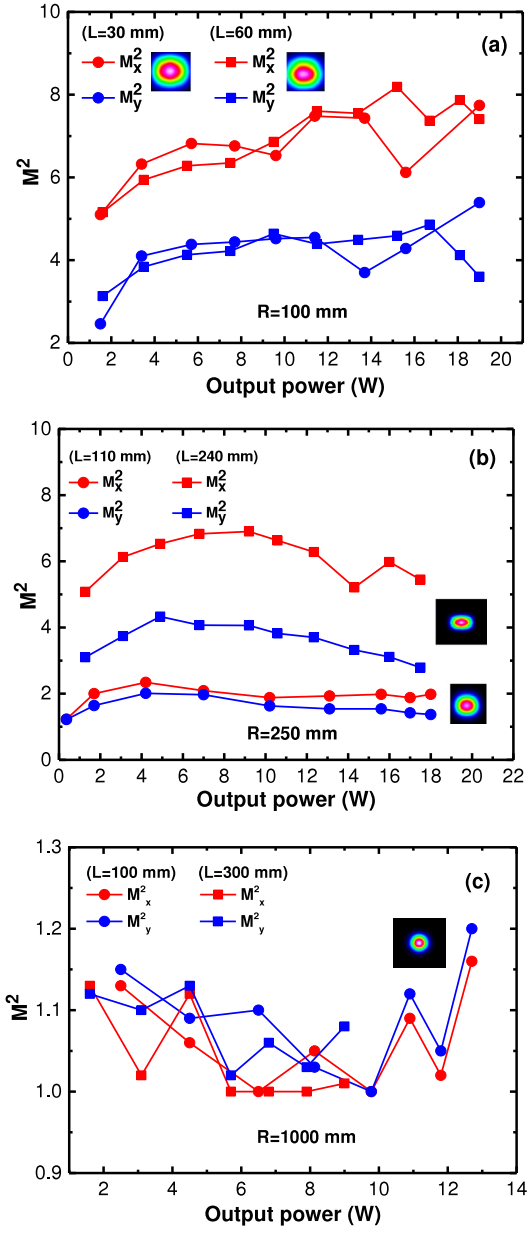

Fig. 8. The output power dependent M^2 factors for (a) R = 100 mm (b) R = 250 mm (c) R = 1000 mm. Insets: the beam profiles recorded at each maximum output power. The beam profile in (c) refers to L = 100 mm.

beam quality factors for both cavity lengths increase with output power in generally. They are almost equal to each other both in x and y directions. However, at around the maximum output power, M^2 of the SDL with L = 60 mm becomes better than that of L = 30 mm especially in y direction. The M^2 fluctuation in higher output power maybe due to mode hopping. In contrast, the beam quality of the SDL with L = 30 mm get worst under maximum output power. The M^2 values under high power (>10 W) are overall in the range of 6 to 8.2 M^2_y for and in the range of 3.6 to 5.4 for M^2_y.

If increasing R to 250 mm, the beam quality becomes better than that of R = 100 mm as shown in Fig. 8(b), which are less than 5.5 (M^2_x) and 2.8 (M^2_y) at the maximum output power. The beam quality of L = 240 mm is much worse than L = 110 mm in both x and y directions. Better beam quality is obtained for L = 110 mm, which is in the range of 1.23 to 2.35.

Fig. 8(c) shows the beam quality of SDL with OC's curvature radius of 1000 mm. The beam quality for the two different cavity lengths L = 100 mm and 300 mm are measured. The M^2 of the two cavity lengths are both less than 1.2 at their respective maximum output powers. The fluctuation in Fig. 8(c) is owing to the measurement error in the range of 1 to 1.2. The maximum power with $M^2 \leq 1.2$ is 12.9 W.

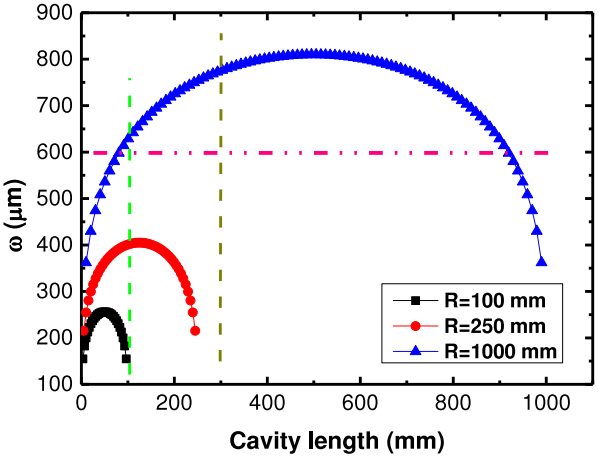

Fig. 9. Mode spot diameters for SDL with the OC curvature radius of R = 100 mm, 250 mm and 1000 mm as function of cavity length.

In order to understand the factors and mechanism affecting the beam quality of the SDL, a deep insight on the relationship between the pump spot size and the mode diameter on the gain chip was performed. The $1/e^2$ diameters of fundamental TEM_{00}mode ω on the semiconductor chip in the planar-spherical cavity can be described as follow [23]

$$\omega^2 = \frac{4\lambda L}{\pi}\sqrt{(R-L)/L}, \quad (1)$$

where λ is the wavelength of SDL, L is the cavity length and R is the curvature radius of OC. The calculated dependence of ω on the cavity length L was plotted in Fig. 9 for R = 100 mm (squares), 250 mm (circles) and 1000 mm (triangle). The pink dash line stands for the pump spot diameter of 600 μm. As can be seen, the diameters of TEM_{00}mode increase with the cavity length, which would decrease after reaching their largest values at L = R/2. Additionally, larger R means a higher available fundamental mode diameter. The mode diameters of SDLs for R = 1000 mm with L = 100 mm and 300 mm are 626 μm and 775 μm respectively. Based on the results shown in Fig. 8(c), it means that the larger mode diameter, the better M^2 factor. To describe the relationship between the diameters of TEM_{00}mode and the beam quality, we defined A as the ratio between the diameter of TEM_{00}mode and pump spot size, which was plotted in Fig. 10. Just as shown in Fig. 10, the beam quality improves with the increase of A, and near-diffraction-limitation level (average value of M^2<1.2) is achieved when A is around 1.04 to 1.3. The average value of M^2 is calculated by the Thorlabs Beam Analyzing Software. Furthermore, the value of A was suggested to be 1.2 for SDL according to Ref. [24], which is in a good agreement with our results. Hence, choosing the pump spot size 10% to 20% smaller than the TEM_{00}mode size is the roughly optimized condition for the purpose of stable and near-diffraction limited beam quality in SDLs. Actually, the accurate and quantitative description on this rule is difficult because the pump spot is just nominally circular shape. In the experiment, it is not as perfectly circular or perfectly homogeneous as the flat top profile [25] assumed in the theory due to the incident angle, thermal lensing effect and inhomogeneous density distribution in the spot. In part, this also causes the inhomogeneous pump profile. The center of the pump spot has a somewhat higher pump power that can push that area above threshold before the whole pump spot area contributes to lasing. These effects lead to a reduced threshold and efficiency just above the threshold.

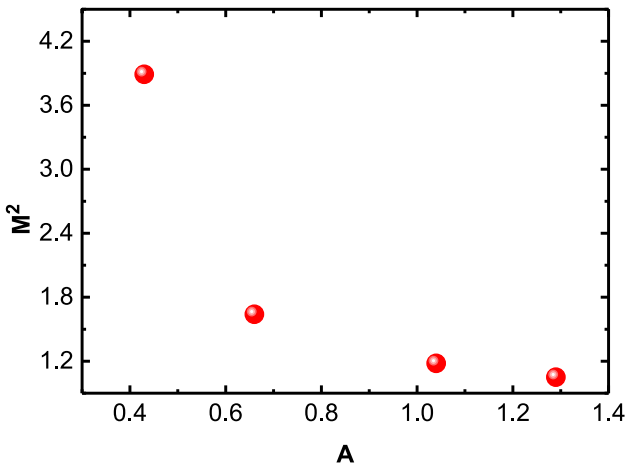

Fig. 10. The dependence of beam quality M^2 factor (average value) on the ratio A of the fundamental mode diameter and pump spot diameter. The average values of the M^2 calculate from the beam qualities of the maximum output powers in Fig. 8(b) and (c).

4. Conclusion

In summary, we had demonstrated a high power SDL (12.9 W) with near-diffraction limited (M^2<1.2) beam quality. The influence of cavity length and curvature radius of the OC mirror on the beam quality were investigated in detail. It was found when the ratio between the fundamental mode diameter and the pump spot diameter was around 1.0.4 to 1.3, the SDL tends to operate with near-diffraction limited beam quality. The mechanism behind was analyzed. We believe these results would contribute the development of high power and high beam quality SDL.

Acknowledgments

This work was supported by TRUMPF GmbH, Germany, in part by National Natural Science Foundation of China (Nos. 61790584).

References

[1] M.R. Johnson, N. Holonyak Jr, Optically pumped thin-platelet semiconductor lasers, J. Appl. Phys. 39 (1968) 3977, http://dx.doi.org/10.1063/1.1656883.
[2] H. Le, S. Di Cecca, A. Mooradian, Scalable high-power optically pumped gaas laser, Appl. Phys. Lett. 58 (1991) 1967, http://dx.doi.org/10.1063/1.105034.
[3] S.L. Shu, G.Y. Hou, J. Feng, L.J. Wang, S.C. Tian, C.Z. Tong, L.J. Wang, Progress of optically pumped GaSb based semiconductor disk laser, Opto-Electron. Adv. 1 (2) (2018) 170003, http://dx.doi.org/10.29026/oea.2018.170003.
[4] M. Kuznetsov, F. Hakimi, R. Sprague, A. Mooradian, Design and characteristics of high-power (> 0.5-W CW) diode-pumped vertical-external-cavity surface-emitting semiconductor lasers with circular TEM00 beams, IEEE J. Sel. Top. Quantum Electron. 5 (1999) 561, http://dx.doi.org/10.1109/68.605500.
[5] W. Jiang, S. Friberg, H. Iwamura, Y. Yamamoto, High powers and subpicosecond pulses from an external-cavity surface-emitting InGaAs/InP multiple quantum well laser, Appl. Phys. Lett. 58 (1991) 807, http://dx.doi.org/10.1063/1.104495.
[6] M. Kuznetsov, F. Hakimi, R. Sprague, A. Mooradian, High-power (> 0.5-W CW) diode-pumped vertical-external-cavity surface-emitting semiconductor lasers with circular TEM00 beams, IEEE Photon. Technol. Lett. 9 (1997) 1063, http://dx.doi.org/10.1109/68.605500.
[7] J. Sandusky, S. Brueck, A CW external-cavity surface-emitting laser, IEEE Photon. Technol. Lett. 8 (1996) 313, http://dx.doi.org/10.1109/68.481101.
[8] T.L. Wang, Y. Kaneda, J.M. Yarborough, J. Hader, J.V. Moloney, A. Chernikov, S. Chatterjee, S.W. Koch, B. Kunert, W. Stolz, High-power optically pumped semiconductor laser at 1040 nm, IEEE Photon. Technol. Lett. 22 (2010) 661, http://dx.doi.org/10.1109/LPT.2010.2043731.
[9] D.A. Nakdali, M. Gaafar, M. K.Shakfa, F. Zhang, M. Vaupel, K.A. Fedorova, A.R. Iman, E.U. Rafailov, M. Koch, High-power operation of quantum-dot semiconductor disk laser at 1180 nm, IEEE Photon. Technol. Lett. 27 (2015) 1128, http://dx.doi.org/10.1109/LPT.2015.2408619.
[10] D.A. Nakdali, M.K. Shakfa, M. Gaafar, M. Butkus, K.A. Fedorova, M. Zulonas, M. Wichmann, F. Zhang, B. Heinen, A.R. Iman, W. Stolz, E.U. Rafailov, M. Koch, High-power quantum-dot vertical-external-cavity surface-emitting laser exceeding 8 W, IEEE Photon. Technol. Lett. 26 (2014) 1561, http://dx.doi.org/10.1109/LPT.2014.2329269.
[11] A.V. Shchegrov, D. Lee, J.P. Watson, A. Umbrasas, A. Mooradian, 490-nm coherent emission by intracavity frequency doubling of extended cavity surface-emitting diode lasers, Proc. SPIE 4994 (2003) 197, http://dx.doi.org/10.1117/12.475743.
[12] Robert G. Bedford, Tuoc Dang, David Tomich, Recent VECSEL developments for sensors applications, Proc. SPIE 8242 (2012) 82420W, http://dx.doi.org/10.1117/12.910607.
[13] B. Rudin, A. Rutz, M. Hoffmann, D.J.H.C. Maas, A.-R. Bellancourt, E. Gini, T. Südmeyer, U. Keller, Highly efficient optically pumped vertical-emitting semiconductor laser with more than 20 w average output power in a fundamental transverse mode, Opt. Express 33 (2008) 2719, http://dx.doi.org/10.1364/OL.33.002719.
[14] H.C. Meng, T.Y. Sun, H. Tan, J.H. Yu, W.C. Du, F. Tian, J.M. Li, S.X. Gao, X.J. Wang, D.Y. Wu, High-brightness spectral beam combining of diode laser array stack in an external cavity, Opt. Express 23 (2015) 21819, http://dx.doi.org/10.1364/OE.23.021819.
[15] Y.F. Zhao, F.Y. Sun, C.Z. Tong, S.L. Shu, G.Y. Hou, H.Y. Lu, X. Zhang, L.J. Wang, S.C. Tian, L.J. Wang, Going beyond the beam quality limit of spectral beam combining of diode lasers in a v-shaped external cavity, Opt. Express 26 (11) (2018) 14058, http://dx.doi.org/10.1364/oe.26.014058.
[16] A. Chernikov, J. Herrmann, M. Koch, B. Kunert, W. Stolz, S.Chatterjee, S.W. Koch, T.L. Wang, Y. Kaneda, J.M. Yarborough, J. Hader, J.V. Moloney, Heat management in high-power vertical-external-cavity surface-emitting lasers, IEEE J. Sel. Top. Quantum Electron. 17 (2011) 1772, http://dx.doi.org/10.1109/JSTQE.2011.2115995.
[17] A. Harkonen, S. Suomalainen, E. Saarinen, L. Orsila, R. Koskinen, O. Okhotnikov, S. Calvez, M. Dawson, 4 w single-transverse mode VECSEL utilising intra-cavity diamond heat spreader, Electron. Lett. 42 (2006) 693, http://dx.doi.org/10.1049/el:20060462.
[18] K. Ursula, A.C. Tropper, Passively mode locked surface-emitting semiconductor lasers, Phys. Rep. 429 (2006) 67, http://dx.doi.org/10.1016/j.physrep.2006.03.004.
[19] J.D. Berger, D.W. Anthon, A. Caprara, J.L. Chilla, S.V. Govorkov, A.Y. Lepert, W. Mefferd, Q.Z. Shu, L. Spinelli, 20 watt CW TEM00 intracavity doubled optically pumped semiconductor laser at 532 nm, Proc. SPIE 8242 (2012) 824206, http://dx.doi.org/10.1117/12.907511.
[20] A. Laurain, M. Myara, G. Beaudoin, I. Sagnes, A. Garnache, Multiwatt-power highly-coherent compact single-frequency tunable vertical-external-cavity-surface-emitting-semiconductor-laser, Opt. Express 18 (2010) 14627, http://dx.doi.org/10.1364/OE.18.014627.
[21] M. Mueller, N. Linder, C. Karnutsch, W. Schmid, K.P. Streubel, J. Luft, S.-S. Beyertt, A. Giesen, G.H. Doehler, Optically pumped semiconductor thin-disk laser with external cavity operating at 660 nm, Proc. SPIE 4649 (2002) 265, http://dx.doi.org/10.1117/12.469242.
[22] G.Y. Hou, S. Shu, J. Feng, Andreas. Popp, Berthold. Schmidt, H.Y. Lu, L.J. Wang, S.C. Tian, C.Z. Tong, L.J. Wang, High power (>27 W) semiconductor disk laser based on pre-metallized diamond heatspreader, IEEE Photon. J. 11 (2019) 1, http://dx.doi.org/10.1109/JPHOT.2019.2908876.
[23] O.G. Okhotnikov, Semiconductor Disk Lasers: Physics and Technology, John Wiley & Sons, 2010.
[24] F. Zhang, B. Heinen, M. Wichmann, C. Möller, B. Kunert, A.R. Iman, W. Stolz, M. Koch, A 23-watt single-frequency vertical-external-cavity surface-emitting laser, Opt. Express 22 (2014) 12817, http://dx.doi.org/10.1364/OE.22.012817.
[25] A. Chernikov, J. Herrmann, M. Scheller, M. Koch, B. Kunert, W. Stolz, S. Chatterjee, S.W. Koch, T.L. Wang, Y. Kaneda, J.M. Yarborough, J. Hader, J.V. Moloney, Influence of the spatial pump distribution on the performance of high power vertical-external-cavity surface-emitting lasers, Appl. Phys. Lett. 97 (2010) 191110, http://dx.doi.org/10.1063/1.3515911.